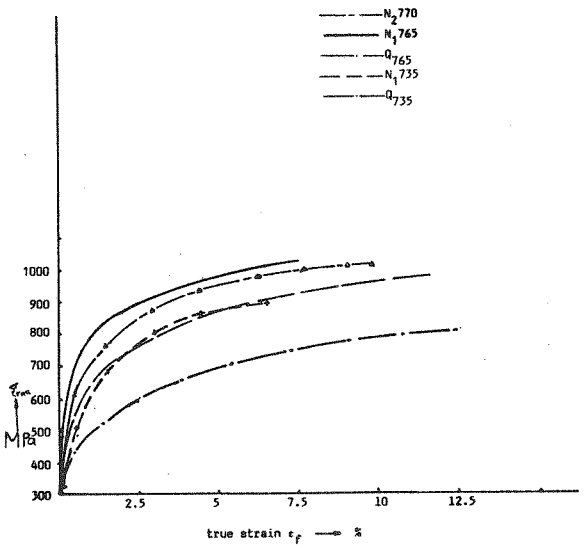

Fig.3.18. True stress-strain curves for all the series.

4. CONCLUSIONS

Based on a study of tensile and fatigue resistance in En14 steel, intercritically annealed at 735°C, 765°C, and 770°C with different initial microstructures, the following conclusions were made.

1– Intercritical annealing and brine quenching of the normalized microstructures resulted in equiaxed ferrite grains with a martensite network along the grain boundary. After the higher normalizing temperature, the microstructure was coarser.

2– Intercritical annealing of the quenched and tempered microstructure resulted in an inhomogeneous grain size of ferrite and non-uniform distribution of martensite. In the coarse-grained regions of samples annealed at 735°C, intragranular cementite particles were still present after heat treatment, in addition to the martensite network on ferrite grain boundaries. The stability of the cementite may have been due to the segregation of Mn to them during coarsening in the tempering treatment.

3– In agreement with Sherman et al (3), it was found that the fatigue limit of dual phase steel increased with martensite content, and the amount of the increase was more significant for the quenched and tempered initial microstructure.

4– The fatigue limit of the coarse normalized initial microstructure $N_2$770 was similar to that of the finer normalized microstructure, $N_1$765, and they were superior to the fatigue limits of specimens which had the quenched-tempered initial microstructures. At high stress amplitude, the coarse normalized initial microstructure was superior due to its combination of high strength, high work hardening rate and fairly good ductility.

5– The tensile properties of specimens derived from the coarse, normalized initial microstructure exhibited a combination of high strength, greater early work hardening rate, and intermediate ductility, in comparison with the other series.

6– Specimens Q_{735}, Q_{765} and $N_2$770 exhibited three stages of deformation, and their terminal work hardening indices, n_3, were nearly equal to the uniform true strain, e_u; these specimens were more ductile than those of the N_1 Series. Specimens which were normalized at 900°C before dual phase heat treatment were less ductile and exhibited only two stages of deformation. In these cases, $e_u < n_3$.

7– Examination of fatigue fracture surfaces revealed, striations, secondary cracks, and cleavage facets in ferrite. Cleavage was more common in the coarse microstructures near the transition from stage II to final fracture, and during final fracture.

SUGGESTIONS FOR FURTHER WORK

1– Correlation of fatigue crack initiation with various microstructures of dual phase steel in a different range of stresses, may be a topic for a new research project.

2– It would be useful to study the effect of mean ferrite path and martensite particle size on fatigue and tensile properties of dual phase steels made from homogenized material.

References

1. R. D. Lawson, D. K. Matlock, G. Krauss, Metallography 1980, Vol. 13. P. 71–78
2. S. Estay, L. I. Chngji, G. R. purdy, can. Met. Q., 1984 Vol. 23, P. 121.
3. A. M. Sherman and R. G. Davies, int. J. Fatigue, Jan 1981, P. 36.
4. T. Ishihara, Journal of Reinforced plastics and composites, Vol. 2, April 1983.

As illustrated in Fig. (3.17) cleavage became a major fracture mechanism in specimens which had the $N_2$770 initial microstructure. Ishihara (4) suggested cleavage cracking of ferrite in coarse-grained dual phase steel is due to internal stresses associated with the phase transformation of austenite to martensite and plastic constraint during the loading due to the presence of the hard second phase.

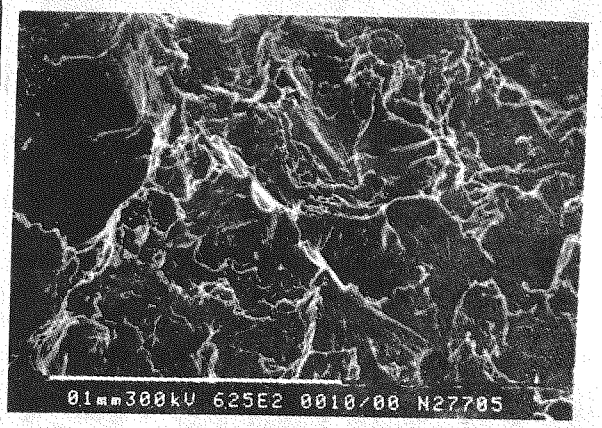

Fig.3.17. Scanning electron micrograph showing cleavage facets as a major fracture mechanism, $N_2$770 Series. S= 385 NPa, x350

3.4 Tensile Properties

3.4.1 Stress-strain curves

The tensile properties at room temperature of spacimens with different microstructures are listed in Table (3.2.). Typical true stress-true strain curves up to the onset of necking are shown in Fig. (3.18). Specimens of Series $N_1$765 had the highest, and Series Q_{735} the lowest Yield and ultimate stresses. The initial work hardening rate is greatest in $N_1$765 and is least in Q_{735}, but the uniform and total elongation of the latter is greatest. Coarse normalised initial microstructure, $N_2$770, resulted in a combination of high strength, one of the highest early work hardening rates, and an intermediate ductility in comparison with the other microstructures.

The superior properties of $N_2$770 specimen may also be related to a less banded microstructure resulting from the high temprature of normalizing (1100), compared with other microstructures (900°C).

Table 3.2. Tensile Properties

Property \ Series	Q_{735}	Q_{765}	$N_1$735	$N_1$765	$N_2$770
true stress $\sigma_{0.1\%}$	339	408	325	391	377
true stress $\sigma_{0.2}$	375	455	397	479*	473
true stress σ_u	812	985	890	1029	1017
U.T.S.*	717	877	836	955	926
U.T.S. average	702	830	761	893	925
ϵ_u %	12.4*	11.6*	6.29	7.46	9.85
e_u average	11.2	11.26	6.76	8.03	9.7
ϵ_t %	15.6*	12.9*	11.5	9.8	12.2
Hardness V.H.	180	231	234	260	281
Stage No.	1	2	3	1	2	3	2	3	2	3	1	2	3
n	0.15	.24	.14	0.185	.2	.12	0.26	0.15	.28	0.13	0.27	.16	0.1'
Strain interval	(.1--.2)	(.2--1.5)	(1.5--11.5)	(.1--.5)	(.5--6.5)	(6.5--11.5)	(.1--3)	(3--6.5)	[(.1--3)	(3--7.5)]	[(.1--1.5)	(1.5--8)	(8--10)]
$\sigma_{U.T.S.}/\sigma_{0.1}$		2.07			2.04			2.34		2.28			2.45

* Best specimen property.

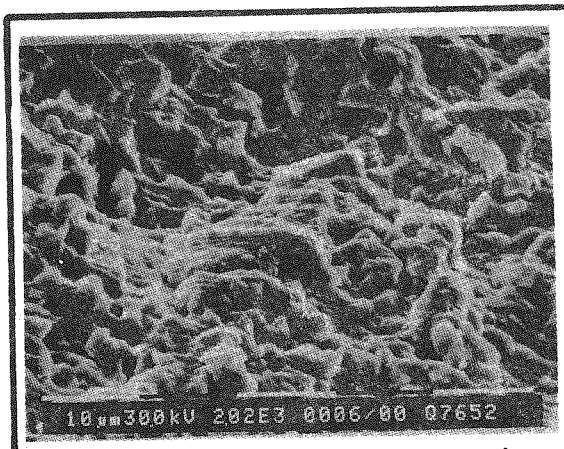

Fig.3.11. Scanning electron mictograph showing striations and secondary cracks,Q765 Series. S=413 MPa. x1100

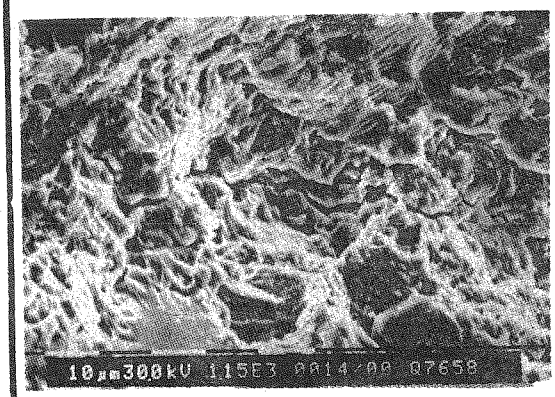

Fig. 3.12. Scanning electron micrograph showing transition from Stage II to Stage III, Q_{765} Sample, ΔS = 475 MPa. Ductile dimples, secondary cracks, striations, cleavage facets. x625

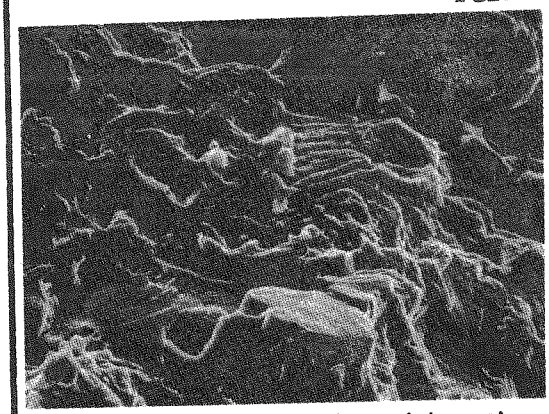

Fig.3.13. Scanning electron mictograph showing transition from StageII to Stage III,$N_2$770 Sample,ductile dimples, secondary cracks, striations,cleavage facets. S=414 MPa. x700

Fig.3.14. Scanning electron micrograph showing final fracture,shear liP,elongated dimples,$N_1$735. S= 392 MPa. x1500

At the higher martensite contents also, the finer microstructure exhibited a more ductile appearance. Fig.(3.15) of a Q_{765} sample shows completely ductile dimples, while Fig. (3.16) shows some cleavage facets.

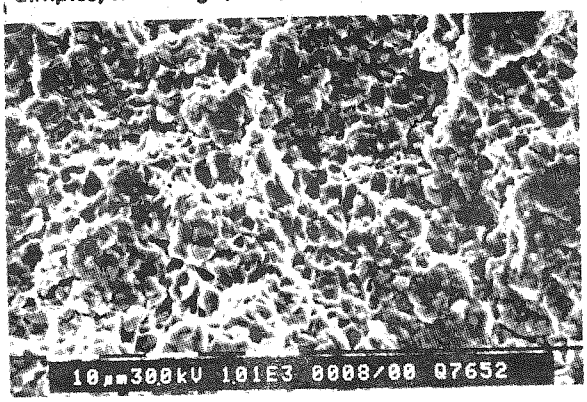

Fig.3.15. Scanning electron micrograph showing ductile dimles,Q765. S=413 MPa. x600

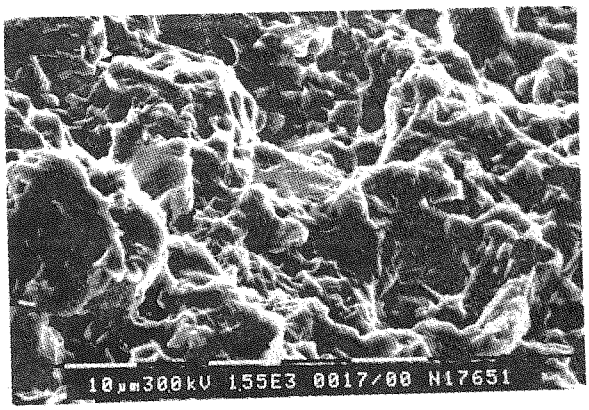

Fig. 3.16.Scanning electron micrograph showing ductile dimples,cleavage facete$N_1$765 Sample. S=401 MPa. x750

Table 3.1. Fatigue Properties

Property \ Series	Q_{735}	Q_{765}	N_1735	N_1765	N_2770
1. Fatigue limit MPa	318	344	383	384	383
2. Fatigue ratio = Fatigue Limit / Tensile Strength	0.39	0.35	0.43	0.37	0.376
3. Fatigue Limit / Proof Stress (0.1%)	0.94	0.84	1.18	0.98	1.02

The long life fatigue data for the 5 series of dual-phase steel investigated in this work, are summarized in Table (3.1).

It can be seen that:

1— Fatigue ratio (F.L./U.T.S.) (for all the series), is considerably lower than would be expected for low and medium carbon steel (i.e. F. R.≃0.50).
2— Fatigue ratio is higher for the coarser microstructures at both levels of martensite content (23% and 40%).
3— Fatigue ratio decreases strongly with increasing strength (Martensite content).
4— From Table (3.1) fatigue ratio (F.L./O. 1% Proff. Stress) for all the series is ≃ 1.

Considering these results, it is concluded that the low proff stress of dual phase steel strongly limits their fatigue limit despite their high work hardening rate in the early stage of plastic deformation, and despite their high U.T.S., and high U.T.S./ Proof Stress ratio.

3.3. Fractography

Scanning electron microscopy of fatigue specimen fracture surfaces indicated that crack initiation typically began from near the specimen surface. In Figure (3.9) the crack is thought to have initiated from an inclusion near the surface of the specimen. In Fig. (3.10), and Fig. (3.11) striations and secondary cracks for the Series N_1765, and Q_{765} are shown. The transition from stage II fatigue crack propagation to final ductile fracture are seen in Fig. (3.12) of Series Q_{765}, and in Fig. (3.13) of the specimen N2770. Striations, sercondary cracks, ductile dimples, and cleavage facets are present in the same photograph.

Elongated dimples related to the last part of fracture (shear lip) of the Series N_{735}, are shown in Fig. (3.14).

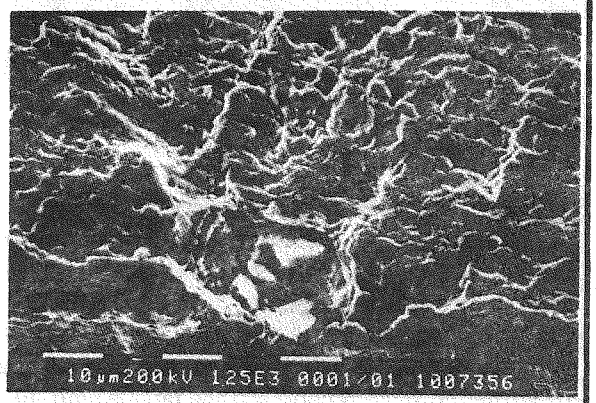

Fig. 3.9. Scanning electron micrograph of crack origin N_1735 fatigue fracture specimen. S= 469 MPa.
×780

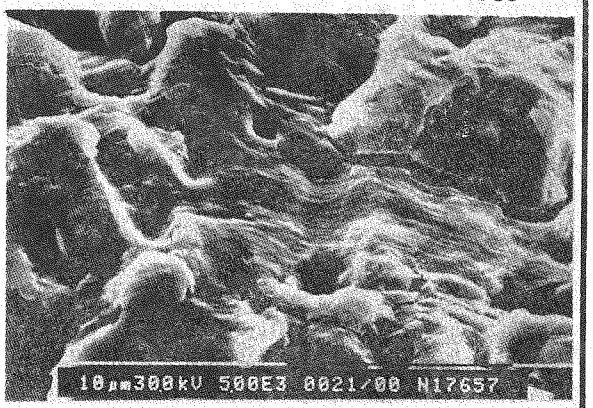

Fig.3.10. Scanning electron micrograph showing striations and secondary cracks.N765 Series. S=389 MPa.
×2700

Intercritical annealing at 765°C tended to reduce the difference between the two regions of the duplex microstructure developed after intercritical annealing at 735°C. Firstly, all the cementite dissolved at the higher temperature. Secondly the larger austenite volume fraction present appeared to be more uniformly distributed, Fig (3.5).

Fig. 3.5 .Edge of fatigue test Specimen Q765,Nital etched. ×625

3.2. Load controlled fatigue resistance

Specimens of all the series of different microstructures were tested in rotating-bending fatigue after intercritical annealing at 735°C and 765°C or 770°C, in order to study the effect of morphology and volume fraction of martensite, and of grain size of ferrite, on the S/N curve and the fatigue limit. Fig. (3.6), illustrates the effect of martensite content on the fatigue resistance of specimens which were quenched and tempered prior to dual-phase heat treatment. It is seen that with increasing martensite content, the fatigue limit improved, in agreement with the findings of Davies et al. (3)

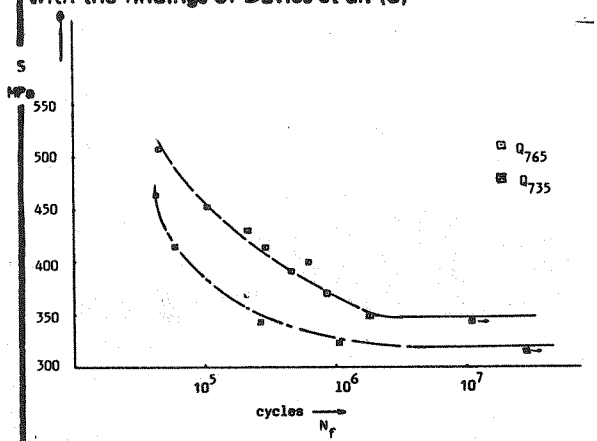

Fig. 3.6. Effect of martensite content on S-N curves for Q Series.

The S/N curves for the three different initial microstructures after dual-phase heat treatment to produce approximately 40% martensite, are compared with each other in Fig. (3.7). These are the N_1 and Q Series intercritically annealed at 765°C and the N_2 Series at 770°C. Clearly the coarser microstructures exhibited the better fatigue limit. It is also seen that at less than 10^5 cycles the endurance of the Q Series was greater than that of the N_1 Series. The S/N curves of various microstructures, investigated in this work are compared in Fig. (3.8).

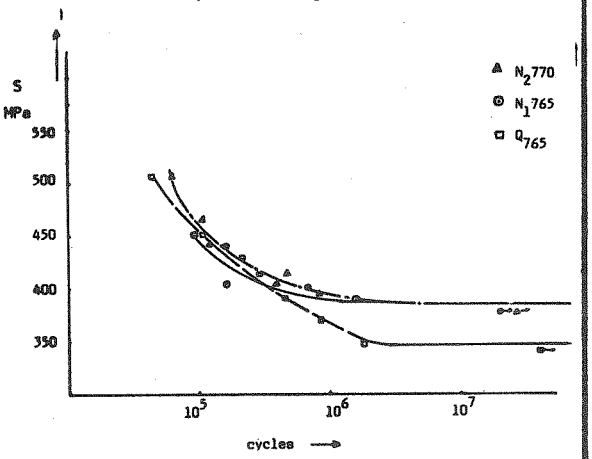

Fig. 3.7. Effect of microstructure on S-N curves for Q765, N_1 765, and $N_2$770.

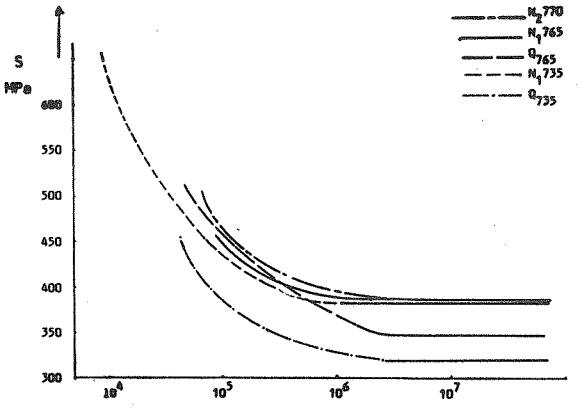

Fig. 3.8. S-N curves for all the series investigated in this work.

As a result it is concluded that the coarser normalized initial microstructure, $N_2$770, is superior in fatigue response due to its high strength, high early stage work hardening rate and relatively good ductility.

3. RESULTS AND DISCUSSION

3.1 Microstructures

(a) Normalized initial microstructure

Figure (3.1) illustrates the type of microstructure obtained by reheating a normalized steel (series N_1) into the ($\alpha + \gamma$) region, partially transforming the microstructure to austenite, and quenching. Intercritical annealing at 735°C produced a microstructure in which the martensite particles form a partial network at ferrite grain boundaries, Fig. (3.1.).

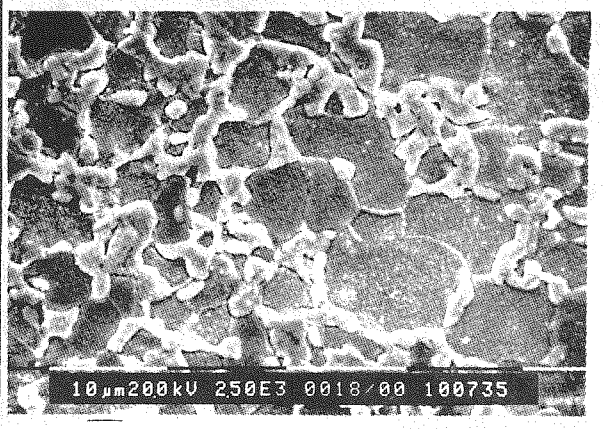

Fig. 3.1. Scanning electron micrograph of dual-phase steel, N_1 Series, intercritically annealed at 735.C, Nital etched. x1400

The specimens of Series N_2, normalized at 1100°C, behaved in a qualitively similar way, but the ferrite grain size was coarser due to the higher, initial normalizing temperature, Fig. (3.2).

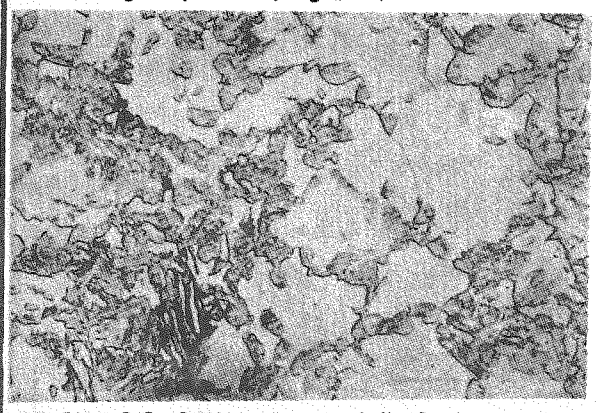

Fig. 3.2. Dual-phase steel, N_2 Series, intercritically annealed at 770, Nital etched. x550

(b) Quenched-Tempered initial microstructure

The result of intercritically annealing this starting microstructure at 735°C, followed by brine quenching is illustrated in Fig. (3.3) and Fig. (3.4). The ferrite-martensite microstructure developed was duplex in nature. that is, during intercritical annealing, in some regions the ferrite grains remained fine and in others the ferrite grains grew to very large dimensions.

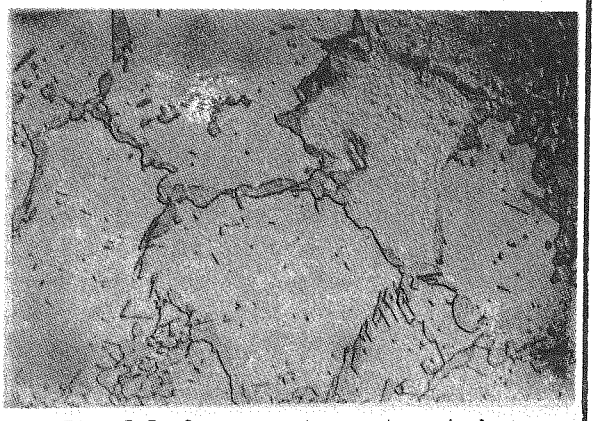

Fig. 3.3. Coarse grain region, dual phase steel, Q735 Sample, Nital etched, x550

In the coarse-grained regions, Fig. (3.3), austenite was formed from the cementite present at ferrite grain boundaries, and grew along the grain boundaries. On quenching this austenite transformed to martensite. Fig. (3.3) shows that a second phase is also present in the form of relatively fine particles within the coarse ferrite grains. Most of these particles are cementite. It has been proposed (2) that during coarsening growing cementite particles become enriched in manganese and this may stabilize them agaist austenite formation.

In the fine grained region, Fig (3.4), martensite formed a nearly continous network at ferrite grain boundaries, and ferrite grain growth was inhibited by austenite formation during intercritical annealing.

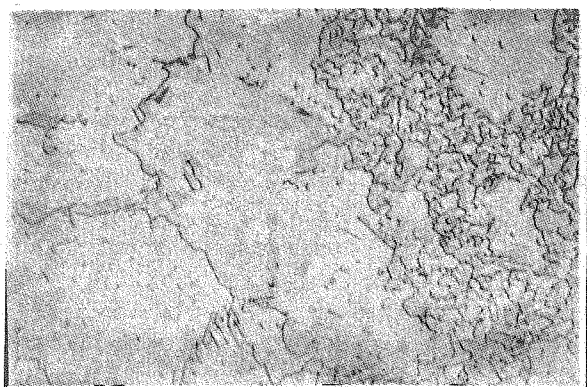

Fig. 3.4. Duplex microstructure, Q735 Sample, Nital etched. x550

2.3. Metallography

For positive phase identification various etchants were used!

1) Immersion in 2% Nital etched ferrite-carbide aggregates (pearlite and bainite) grey, leaving martensite unetched with a bold outline; ferrite grain boundaries were also etched.
2) An etching technique developed by Lawson et al (1) was used to differentiate old and new ferrite. It consisted of etching in 5% Picral followed by immersion in a boiling alkaline chromate solution* (8 g CrO_3 + 40 g NaOH + 72 ml H_2O). Martensite appeared a black or brown colour and the old ferrite was stained a grey/blue colour while the new ferrite was a brilliant white, the boundaries between these two areas of ferrites indicating the extent of the prior austenite pools formed during intercritical annealing, Fig(2.4). Microstructural examinations were performed using both optical and scanning electron microscopes. A Swift point counter was used to determine the volume fraction of each constituent produced from the austenite volumes.

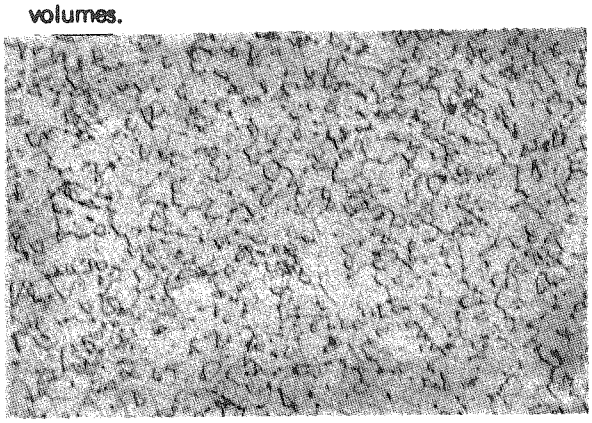

Fig. 2.3. Quenched tempered initial microstructure, ferrite-spheroids' carbide, Nital etched. ×550

2.4. Fatigue testing

Specimens for fatigue tests were machined from the heat treated blanks, to the dimensions shown in Fig. 2.5, then polished so that no transverse machining or polishing marks should be visible.

Fatigue testing was done using a rotating-bending, constant-load Wohler testing machine of 2850 r.p.m. The test environment was laboratory air with relative humidity in the range 45–60%, and temperatures in the range of 10–22°C.

The fractured surface of fatigue specimens were cleaned with diethyl ether and examined in a Philips 505 scanning electron microscope.

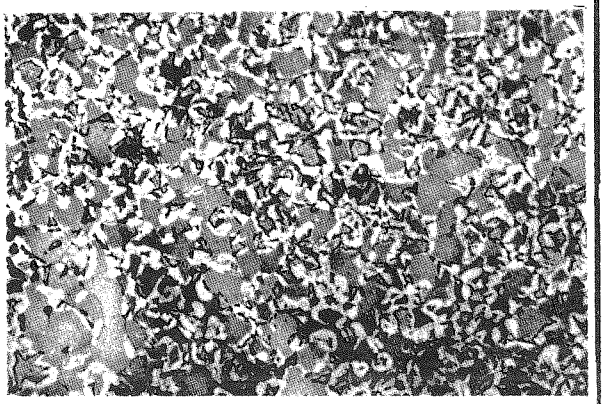

Fig. 2.4 Dual-phase steel, M_1 Series, intercritically annealed at 605.C. alkaline chromate etched. Showing epitaxial ferrite (white), old ferrite (grey), and martensite(black). ×550

2.5. Tensile testing

After heat treatment, the blanks were machined into tensile samples with gauge sections 4.54 mm in diameter and 38.1 mm long. All tensile tests were conducted at a strain rate of 0.1 per minute to half percent strain and then at a strain rate of 0.5 per minute to failure, using a microprocessor-controlled Instron testing machine.

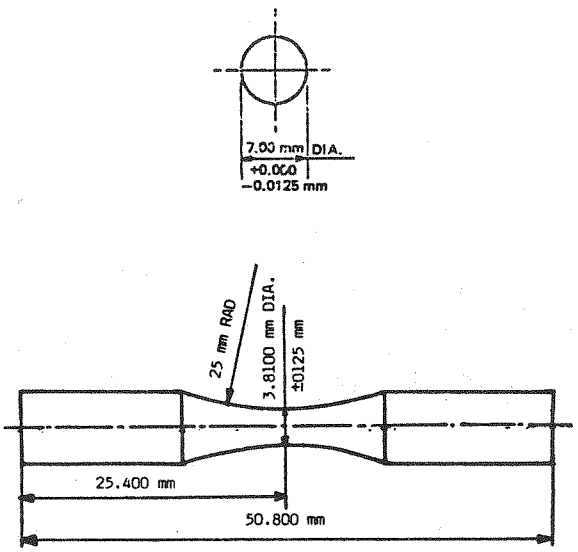

Fig.2.5. Rotating-bending test specim.

* Appropriate safety precautions should be observed, because the addition of CrO_3 to aqueous NaOH produces a strong exothermic reaction.

Table 2.1

Elements	C	Si	Mn	P	S	Cr	Mo	Ni	Al	Cu	Nb	V
BSC analysis	0.12	.24	1.31	.024	.007	.10	.02	0.10	.015	.16	0.035	<.01
D.M. analysis	0.13	.34	1.6	.023	.009	.3	.087	0.10	.05	.28	.057	.009

B.S.C. Analysis carried out at Swinden Laboratories

D.M. Analysis carried out at Department of Metallurgy

2.2. Heat treatment

The heat treatment was designed to study the effect of initial microstructure and volume fraction of martensite on the fatigue and tensile properties of dual phase steel. Therefore, the blanks were divided into three series for primary heat treatment in order to obtain a variety of initial microstructures. In series N_1, the blanks were normalized at 900° C for 15 mins, then cooled in a bed of vermiculite to give an equiaxed ferrite-pearlite structure, Fig. 2.1. In Series N_2 the blanks were annealed at 1100° C for 15 mins., then cooled in vermiculite to give a coarse ferrite-pearlite structure, Fig. 2.2. In series Q, the blanks were reaustenitized for 15 mins. at 900° C, and quenched into water at 20°C, then tempered at 700°C for 10 hrs, to give a microstructure of spheroidal carbide in the ferrite matrix, Fig.2.3. Finally, all the above series were then intercritically annealed for 30 mins. at temperatures of 735°, 765°, (and 770°C for N_2), and quenched into 10% brine at − 8°C. Table 2.2. These blanks were then machined to fatigue and tensile test specimens after cutting a piece off the end of each for metallographic examination.

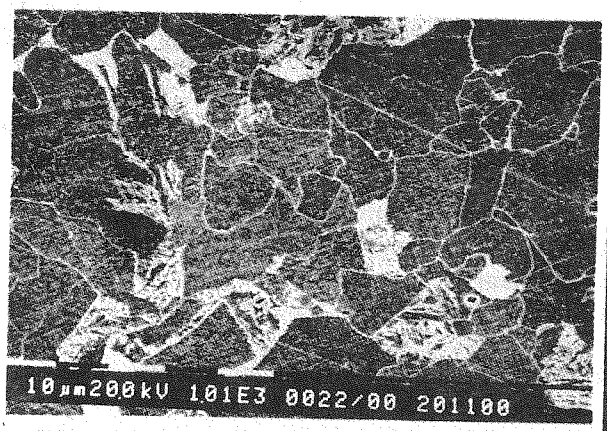

Fig. 2.2. Scanning electron micrograph— showing coarse ferrite-pearlite microstructure, N_2 Series. Metal etched. ×550

Table 2.2

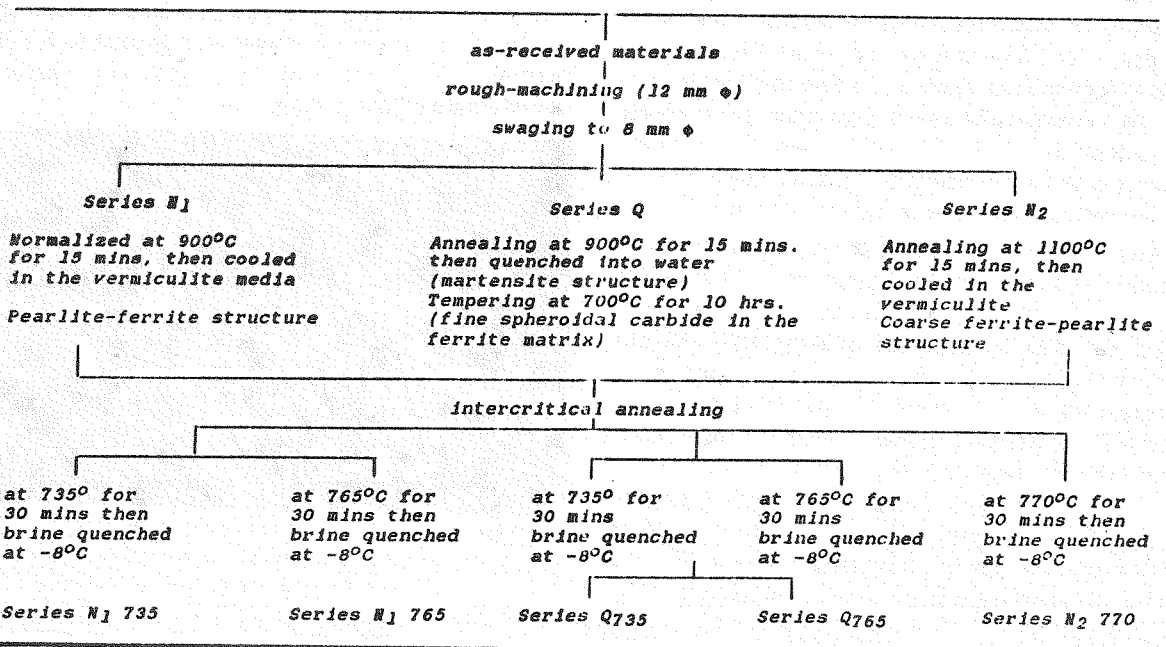

The Effect of Heat Treatment on Fatigue and Tensile Properties of Dual-phase steel

A. Fallahi, M. Sc
Mech. Eng. Dept. Amirkabir Univ. of Tech.

ABSTRACT

The objective of this work was to investigate the effect of microstructure (morphology and grain size), and volume fraction of martensite on fatigue and tensile properties of dual-phase steel. A steel containing 0.12%C, 1.45%Mn, 0.3%Si, 0.2%Cr and 0.045%Nb was heat treated to produce starting microstructures of ferrite-pearlite, coarse ferrite-pearlite, and ferrite-cementite. Each was then inter-critically annealed and brine-quenched. S/N data were obtained in rotating bending. The fatigue limit increased with martensite content and was highest in those samples having the coarser microstructures.

At the same strength level the finer dual-phase microstructures resulting from initial quenching and tempering had the best ductility.

Fractographic examination showed that cleavage facets become more common at the end of fatigue processes, the coarser the microstructure, and the higher the martensite content.

1. INTRODUCTION

From the standpoint of energy efficiency in automobiles it is desirable to use high strength steels to reduce structural weight. However, the higher the strength of steel, the lower its ductility and formability. The development of more ductile high strength dual-phase steels could help to alleviate some of the formability problems. Dual-phase steels consist of a mixture of 15–25% of martensite in a ferrite matrix with a grain size of 5–15 μm. These steels are produced by heating low carbon (-0.1 pct C) steel sheet into the intercritical ($\alpha + \gamma$) phase field, and cooling at a rate so as to produce the desired microstructure containing 15–25% martensite. Dual phase steel can also be obtained directly from the hot-rolling mill, by control of composition and processing. These steels exhibit continuous yielding behaviour, a low 0.2% offset yield strength, a high ultimate tensile strength and a high ductility.

This study has been made of the effect of different martensite morphologies and of volume fraction of martensite on fatigue and tensile properties. The effect of ferrite grain size was also considered.

2. EXPERIMENTAL PROCEDURE

2.1 Material

The steel was received in the form of hot-rolled rod 17 mm in diameter. Its composition is given in Table 2.1. The rod was straightened, then rough machined to 12 mm diameter and swaged to 8 mm diameter. The rod was then cut into blanks, approximately 70 mm long.

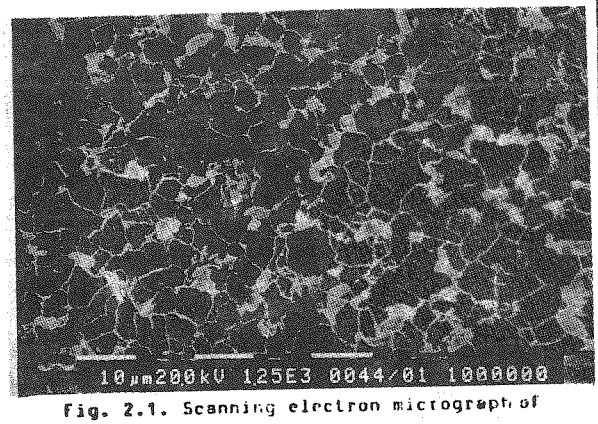

Fig. 2.1. Scanning electron micrograph of normalized initial microstructure, ferrite pearlite N_1 Series, Nital-etched. ×750